# Dnmt3a1 regulates hippocampus-dependent memory via the downstream target Nrp1

Janina Kupke[1], Julien Klimmt[1,2,#], Franziska Mudlaff[1,#], Maximilian Schwab[1] Carsten Sticht[3] and Ana M.M. Oliveira[1,4,*]

[1]Department of Neurobiology, Interdisciplinary Center for Neurosciences (IZN), Heidelberg University, 69120 Heidelberg, Germany

[2]Present address: Institute for Stroke and Dementia Research, University Hospital, Ludwig-Maximilians-University Munich, 81377 Munich, Germany.

[3]Next Generation Sequencing Core Facility, Medical Faculty Mannheim, Heidelberg University, 68167, Mannheim, Germany.

[4]Department of Molecular and Cellular Cognition Research, Central Institute of Mental Health, Medical Faculty Mannheim, Heidelberg University, 68159 Mannheim, Germany

[#]equal contribution

*Ana M.M. Oliveira. Department of Molecular and Cellular Cognition Research, Central Institute of Mental Health, Medical Faculty Mannheim, Heidelberg University, 68159 Mannheim, Germany. Phone: +49(0)62215416510. Email: oliveira@nbio.uni-heidelberg.de, ana.oliveira@zi-manheim.de

**Author Contributions:** JKupke, AMMO designed research; JKupke, JKlimmt, FM, AMMO performed experiments; JKupke, JKlimmt, FM, CS, AMMO analyzed data; JKupke, AMMO wrote the paper. All authors edited the manuscript.

**Abstract**

Epigenetic factors are well established players in memory formation. Specifically, DNA methylation is necessary for the formation of long-term memory in multiple brain regions including the hippocampus. Despite the demonstrated role for DNA methyltransferases (Dnmts) in memory formation, it is unclear whether individual Dnmts have unique or redundant functions in long-term memory formation. Furthermore, the downstream processes controlled by Dnmts during memory consolidation have not been investigated. In this study, we examined the requirement of the predominant Dnmt in the adult brain, Dnmt3a1, for hippocampus-dependent long-term memory formation. Using RNA-sequencing, we identified an activity-regulated Dnmt3a1-dependent genomic program in which several genes were functionally associated with functional and structural plasticity. Our data showed that Dnmt3a1, similarly to its isoform Dnmt3a2, plays a critical role in memory formation and identified Neuropilin 1 (Nrp1) as a downstream target of Dnmt3a1 in this process. Intriguingly, we found that Nrp1 expression is selectively regulated by and a specific downstream effector of Dnmt3a1, but not Dnmt3a2. Taken together, our study uncovered a Dnmt3a-isoform-specific mechanism in memory formation, identified a novel regulator of memory, and further highlighted the complex and highly regulated functions of distinct epigenetic regulators in brain function.

## Introduction

Precise control of gene transcription is required for the functional and structural neuronal remodelling that underlies memory formation and maintenance[1–3]. Gene transcription is orchestrated by the activity of transcription factors[4,5], epigenetic factors, and 3D-genomic factors such as chromatin structure or nuclear organization[6–9]. Indeed, epigenetic mechanisms such as DNA methylation have emerged as important regulators of cognitive processes[8].

DNA methylation has traditionally been viewed as a static mechanism with important roles in transcription repression, cell fate determination, imprinting and silencing of transposons during early development [10]. However, it is now well accepted that DNA methylation plays a critical role in the regulation of genomic responses in mature neurons. Several lines of evidence demonstrated dynamic and quick changes in DNA methylation in response to neuronal activity[11,12] and pharmacological and genetic studies established a causal link between DNA methyltransferase (Dnmt) activity and memory formation. Specifically, the *de novo* DNA methyltransferase, Dnmt3a, plays a documented function in cognitive abilities[13–17]. Furthermore, it has recently been shown that *DNMT3A* variants are the underlying cause of the neurodevelopmental disorder Tatton-Brown-Rahman syndrome, which is characterized by intellectual disability[18,19]. Despite this evidence, the downstream processes regulated by Dnmt3a that contribute to memory formation are unknown. Moreover, the genomic program regulated by Dnmt3a and required for the formation of long-term memory remains uncovered.

The Dnmt3a genomic locus contains two genes, Dnmt3a1 and Dnmt3a2[20], that exhibit different genomic binding[21] and expression regulation in response to neuronal activity. Dnmt3a2 is transcribed from an intronic promoter and behaves like an immediate early gene, whereas the expression of Dnmt3a1 is not regulated by neuronal activity[22–24]. The requirement for Dnmt3a2 in memory formation has been demonstrated[23–25]; however, the contribution of Dnmt3a1, despite its high abundance in the adult brain[26–28] has not been investigated. The differential regulation of expression of the two isoforms by neuronal activity and the studies that showed that normal Dnmt3a1 expression levels do not compensate the memory impairments found in Dnmt3a2 knockdown mice [23,24,29,30], suggest nonredundant functions by the two isoforms. However, whether the two enzymes are differentially required for and regulate distinct downstream processes during memory formation remains to be investigated.

In this study, we demonstrated that Dnmt3a1 is crucial for memory formation and for controlling an activity-regulated genomic program. We found that acute hippocampal reduction of Dnmt3a1 led to memory impairments in adult mice. Moreover, using RNA Sequencing analysis, we identified activity-regulated genes dependent on Dnmt3a1 levels. Intriguingly, we found that some of the identified genes are selectively dependent on Dnmt3a1, but not

Dnmt3a2. Among these genes was Neuropilin-1 (Nrp1), a member of the semaphorin complex with an established function in synaptic plasticity[31,32]. In a next step, we demonstrated the involvement of Nrp1 in hippocampus-dependent memory formation. Furthermore, we showed that Dnmt3a1 regulates hippocampus-dependent memory via Nrp1. In contrast, Nrp1 overexpression did not rescue memory impairments triggered by reduced Dnmt3a2 levels, suggesting an isoform-specific mechanism for memory processes. Taken together these findings uncovered a Dnmt3a1-dependent genomic program and identified a downstream effector during memory formation.

143 **Materials and Methods**

144

145 Animals.

146 In this study, 3-months-old C57BL/6N male mice (Charles River, Sulzfeld, Germany) were
147 used. Mice were housed in groups of 2-3 per cage (except if severe fighting occurred), under
148 a 12h light/dark cycle with *ad libitum* access to water and food, 22 ± 1°C and 55 ± 10% relative
149 humidity. The behavioural experiments were conducted during the light phase. Mice that were
150 sick or injured were excluded. Animals were randomly assigned to experimental groups and
151 analysis was conducted blindly. The procedures complied with German animal care guidelines
152 and European Community Council Directive 86/609/EEC.

153

154 Recombinant Adeno Associated Virus (rAAV) production.

155 Viral particles were produced and purified as described previously[33] and with minor
156 modifications. Briefly, rAAVs were generated by co-transfecting AAV-293 cells (Stratagene
157 #240073, California, USA) with target AAV plasmid and helper plasmids (pFΔ6, pRV1, and
158 pH21) using calcium phosphate precipitation. 60 hours after transfection, the HEK 293 cells
159 were collected and lysed. Remaining viral particles in media were concentrated using 40%
160 Polyethylene glycol (PEG) solution (pH 7,4). For this, the culture medium was added to 40%
161 PEG and stirred for 3h at 4°C. After centrifugation, the viral pellet was added to lysed HEK
162 cells and this was purified through heparin affinity columns (HiTrap Heparin HP, GE
163 Healthcare, Uppsala, Sweden) and concentrated using Amicon Ultra-4 centrifugal filters
164 (Millipore, Bedford, MA). For expression of shRNAs, we used a vector containing the U6
165 promoter upstream of the shRNA sequence and a chicken β-actin promoter to drive GFP
166 expression. The sequences are as following: Dnmt3a1-shRNA1:
167 GCAGACCAACATCGAATCCAT; Dnmt3a1-shRNA2:
168 GGGAGGATGATCGAAAGGAAGGAGA; Dnmt3a2-shRNA:
169 ACGGGCAGCTATTTACAGAGC; Nrp1-shRNA1: GGAAACCAAGAAGAAATATTA; Nrp1-
170 shRNA2: GGGAGAGGAAATCGGAGCTAA; Control-shRNA: ACTACCGTTGTTATAGGTG.
171 For temporally controlled knockdown of Dnmt3a1, we used a dual-component TetON-based
172 system. In detail, this system consisted of a driver plasmid that expresses the transactivator
173 (rtTA), the tetracycline repressor (TetR) and the fluorescent protein Kusabira Orange (KO)
174 that acts as an infection marker under the control of a neuron-specific promoter (hSynapsin).
175 The second construct contains GFP and a miR30-based shRNA targeting Dnmt3a1 under the
176 control of the tetracycline-responsive promoter (TRE). For the generation of this vector, the
177 plasmids pPRIME-CMV-GFP-FF3[34] (a gift from Stephen Elledge (Addgene plasmid # 11663;

178 http://n2t.net/addgene:11663; RRID:Addgene_11663)) and pAAV-PTRE-tight-hM3Dg-
179 mCherry[35] (a gift from William Wisden [Addgene plasmid # 66795;
180 http://n2t.net/addgene:66795; RRID:Addgene_66795]) were used. Specifically, the Dnmt3a1-
181 shRNA1 sequence was inserted into the pPRIME vector and subsequently, the GFP-miR30-
182 Dnmt3a1-shRNA expression cassette was subcloned into the vector containing the Tet-
183 inducible promoter by replacement of the hM3Dq-mCherry insert. For the overexpression of
184 Nrp1-HA or a control gene, we used a vector containing the neuron-specific promoter,
185 hSynapsin, to constitutively express HA-tagged Nrp1 or LacZ, respectively. The infection rate,
186 toxicity, viral titer, and knockdown efficiency for each batch of generated viruses were
187 evaluated. The titer was matched to a final working concentration of around 1-2 $x10^{12}$ viral
188 particles/ml.

189

190 Fluorescent labeling.

191 Deeply sedated mice were perfused intracardially with ice-cold PBS followed by 4%
192 paraformaldehyde (Sigma-Aldrich, Munich, Germany). A post-fixation of the brains with 4%
193 paraformaldehyde solution (Sigma-Aldrich, Munich, Germany) was done overnight at 4 °C.
194 The following day, brains were put in a PBS solution with 30% sucrose and left for three days.
195 Brain slices were cut at a thickness of 30 µm using a cryotome (CM1950, Leica). Slices were
196 incubated in Hoechst 33258 (2 µg/ml, Serva, Heidelberg, Germany) for 5 min, mounted on
197 glass slides and imaged using a 20x oil objective on a TCS SP8 confocal microscope (Leica
198 Microsystems, Oberkochen, Germany).

199

200 Stereotaxic surgery.

201 rAAVs were injected into the dorsal hippocampus (dHPC) at the following coordinates relative
202 to the bregma: -2 mm anteroposterior, ± 1.5 mm mediolateral, -1.7, -1.9 and -2.1 mm
203 dorsoventral from bregma. Each spot received 500 nl of viral solution. Injections proceeded at
204 a speed of 200 nl $min^{-1}$ through a 33G needle. Following injections at each individual site, the
205 needle was left in place for 60 s. At the time of behavioural experiments, the experimenter
206 was blind to the identity of the virus injected into each mouse. Behavioural experiments started
207 3 weeks after rAAV delivery.

208

209 Behavioural testing.

210 Before behavioural testing started, mice were habituated to the experimenter and behavioural
211 room by handling for 3 consecutive days, 1 min/mouse. Different mouse cohorts were used to

212 test short-term (1h) or long-term memory (24h). The spatial object recognition test and
213 contextual fear conditioning were performed as previously described[3]. Briefly, in the object
214 recognition test, mice were habituated to an open arena (50 cm × 50 cm × 50 cm) with a visual
215 cue placed on the arena wall for 6 min, followed by a training session in which mice were
216 exposed to two objects for 6 min over a course of three trials with a 3 min intertrial interval.
217 During the testing session, which occurred 1h or 24h later, one object was moved to a new
218 location and exploration of objects was scored for 6 min. If in one experimental batch during
219 the spatial object recognition test control animals did not show a preference, due to day
220 effects, the whole set of animals was excluded from this analysis but was still included in
221 contextual fear conditioning data. Further, if an animal did not explore the objects during the
222 training for at least 2 seconds, that animal was excluded. One week later, contextual fear
223 conditioning (CFC) was performed. In CFC, mice were allowed to explore the conditioning
224 chamber (23 × 23 × 35 cm, TSE, Bad Homburg, Germany) for 148 s followed by a 2 s foot
225 shock (0.5 mA). They remained for additional 30 s in the conditioning chamber before returning
226 to their home cage (HC). The testing session consisted of exposing the animals to the
227 conditioning chamber for 5 min. For the temporally controlled knockdown of Dnmt3a1, mice
228 received intraperitoneal doxycycline hyclate (2.5 mg in 500 µL saline solution, 100mg/kg,
229 Sigma-Aldrich, Munich, Germany) 3 days prior to CFC.

230

231 Primary hippocampal cultures and pharmacological treatments.

232 Hippocampal cultures from newborn C57Bl/6N mice (Charles River, Sulzfeld, Germany) were
233 prepared and maintained as previously described[3]. In brief, mice hippocampi were dissociated
234 at P0 by papain digestion and plated onto tissue culture dishes coated with poly-D-lysine and
235 laminin (Sigma-Aldrich, Munich, Germany). The primary cultures were maintained for 8 days
236 in Neurobasal-A medium (Gibco™) supplemented with 1% rat serum (Biowest), 0.5 mM L-
237 glutamine (Sigma-Aldrich, Munich, Germany) and B27 (Gibco™), followed by incubation in
238 transfection media: salt-glucose-glycine solution (10 mM HEPES, pH 7.4, 114 mM NaCl,
239 26.1 mM NaHCO3, 5.3 mM KCl, 1 mM MgCl2, 2 mM CaCl2, 30 mM glucose, 1 mM glycine,
240 0.5 mM C3H3NaO3, and 0.001% phenol red) and phosphate-free Eagle's minimum essential
241 medium (9:1 v/v), supplemented with insulin (7.5 µg/ml), transferrin (7.5 µg/ml), and sodium
242 selenite (7.5 ng/ml) (ITS Liquid Media Supplement, Sigma-Aldrich, Munich, Germany) and
243 penicillin-streptomycin. rAAV infection occurred on day in vitro (DIV) 4. Experiments were
244 performed on DIV 9-11. To induce action potential bursting, cultures were treated with 50 µM
245 bicuculline (Alexis Biochemicals, Farmingdale, NY, USA). DNA transfection was performed
246 on DIV 8 using Invitrogen Lipofectamine 2000 (Invitrogen, CA, USA). The DNA (µg):
247 Lipofectamine (µl) ratio was 1.6:5 in 1 ml of medium. The Lipofectamine/DNA mixture was left

248 on the cells for 3 h before it was replaced with a transfection medium. Doxycycline hyclate (25
249 μM, Sigma-Aldrich, Munich, Germany) was introduced in the medium at DIV 8. To monitor
250 doxycycline dependency, images of infected primary neurons with the TetOn-based miR30
251 system were acquired (Axio Vert.A1, Zeiss, Oberkochen, Germany).

252

253 qRT-PCR primer design.

254 The qRT-PCR primers were designed with Primer3 (https://primer3.ut.ee/) using either the
255 RefSeq curated annotation or the GENCODE VM23 comprehensive transcript annotation,
256 along with the GRCm38/mm10 mouse genome assembly. The specificity and amplicon
257 product size of the primers were verified by BLAST search and *in silico* PCR (UCSC Genome
258 Browser, mm10). Primer pair efficiencies and product melting curves were validated by qRT-
259 PCR on serially diluted complementary DNA (cDNA) from primary mouse hippocampal
260 cultures (refer to the "qRT-PCR" section). The list of all primers used in the study is provided
261 in Sup Table 1.

262

263 qRT-PCR.

264 RNA from hippocampal cultures or mouse hippocampal tissue was extracted using the
265 RNeasy Plus Mini Kit (Qiagen, Hilden, Germany) with extra DNase I digestion on the column,
266 following the manufacturer's instructions. For isolation from mouse tissue, the brain was
267 quickly isolated and sliced and the infected region (identified by GFP expression) isolated for
268 RNA extraction. RNA was then transcribed into cDNA using the High-Capacity cDNA reverse-
269 transcription kit (Applied Biosystems, Foster City, CA, USA). Quantitative reverse-transcription
270 PCR (qRT-PCR) was performed on Step One Plus Real-Time PCR System (Applied
271 Biosystems, Foster City, CA, USA) using TaqMan gene expression assays (Applied
272 Biosystems, Foster City, CA, USA) or the Power SYBR Green PCR Master Mix (Applied
273 Biosystems) assays. TaqMan gene expression assays were used for the following target
274 genes: Dnmt1 (Mm00599763_m1), Dnmt3a1 (Mm00432870_m1), Dnmt3a2
275 (Mm00463987_m1), Dnmt3b (Mm00599800_m1) and the housekeeping gene Gusb
276 (Mm00446953_m1). Power SYBR Green PCR Master mix was used for the remaining target
277 genes. PCR reactions were run as technical triplicates in 10 μL reactions (96-well format)
278 using 0.5 μM of each primer. 2 μL of diluted cDNA (about 1.25 ng) was added to each reaction.
279 The thermal cycling was conducted with the following settings: a 10-minute incubation at 95
280 °C, 40 cycles of 10 seconds each at 95 °C, 60 °C, and 72 °C, followed by a 15-second
281 incubation at 95 °C. Melt curves were generated by heating from 60 °C to 90 °C at a ramp

282 rate of 0.6 °C/min. Relative expression levels of each target transcript were determined by the
283 ΔΔCt method using beta-Actin mRNA levels as a reference[36].

284

285 Western Blotting.

286 Primary hippocampal neurons infected on day *in vitro* (DIV) 4 were lysed on DIV 10 in boiling
287 SDS sample buffer (160 mM Tris-HCl (pH 6.8), 4% SDS, 30% glycerol, 10 mM dithiothreitol,
288 and 0.02% bromophenol blue). In the case of western blotting of tissue samples, the dorsal
289 hippocampus was quickly dissected in ice-cold PBS and homogenized in RIPA buffer (150
290 mM NaCl, 1% Triton X-100, 0.5% sodium deoxycholate, 0.1% SDS, 50 mM Tris, pH 8.0)
291 supplemented with 1% protease inhibitor cocktail (Sigma-Aldrich, Munich, Germany). Protein
292 concentration was measured by Bradford assay and 20 µg of denatured protein (in Laemmli
293 buffer at 95°C for 5 min) was loaded in a 7.5% polyacrylamide gel and blotted onto a
294 nitrocellulose membrane (GE Healthcare, Buckinghamshire, UK). The membranes were
295 blocked in 5% milk in phosphate-buffered saline (PBS) with 0.01% Tween (PBST) and probed
296 with the following antibodies (diluted in 5% milk in PBST) overnight at 4 °C: α-Tubulin
297 (1:400000, Sigma t9026), α-Dnmt3a (1:5000, H-295, Santa Cruz, SC-20703), α-HA-tag
298 (1:7500, Covance, MMS101R). The next day, membranes were incubated with horseradish
299 peroxidase-conjugated secondary antibodies (1:5000 diluted in 5% milk in PBST) for 1h at
300 room temperature. Finally, they were analyzed using ChemiDoc™ Imaging System (Bio-Rad,
301 California, USA).

302

303 Immunocytochemistry.

304 Primary hippocampal neurons plated on coverslips were rinsed with PBS and fixed with a
305 prewarmed solution of 4% paraformaldehyde and 4% sucrose for 15 min at room temperature.
306 After permeabilizing the cells in ice-cold methanol for 6 min, blocking was performed with 10%
307 normal goat serum in PBS for 1 h at room temperature. Next, cells were incubated with primary
308 antibody α-Dnmt3a (1:500, H-295, Santa Cruz, SC-20703diluted in PBS containing 2% BSA,
309 0,1% Triton X-100) overnight at 4 °C, which continued with secondary antibody incubation
310 (1:500 goat anti-mouse Alexa488 [Life Technologies, Eugene, OR, USA]) diluted in PBS
311 containing 2% BSA, 0,1% Triton X-100) for 1 h at room temperature. Finally, coverslips were
312 treated with Hoechst 33258 (2 µg/ml, Serva, Heidelberg, Germany) for 5 min and mounted on
313 glass slides. Images were acquired with a 40x oil objective on a fluorescence microscope
314 (Leica Microsystems, Oberkochen, Germany).

315

316 Bulk RNA Sequencing.

317 Total RNA from mouse hippocampal cultures was isolated as above described. 500ng of total
318 RNA from each sample was used for bulk RNA-sequencing analysis. Data processing was
319 performed with R (version 3.6.3) and bioconductor (version 3.9) in Rstudio (version 1.1.463).
320 Quality control of clean sequencing reads was performed using FastQC (Babraham
321 Bioinformatics). Low-quality reads were removed using trim_galore (version 0.6.4). The
322 resulting reads were aligned to the mouse genome version GRCm38.p6 and counted using
323 kallisto version 0.46.1 [37]. The count data were transformed to log2-counts per million (logCPM)
324 using the voom-function from the limma package[38]. Differential expression analysis was
325 performed using the limma package in R. A false positive rate of α= 0.05 with FDR correction
326 was taken as the level of significance. Volcano plots and heatmaps were created using ggplot2
327 package (version 2.2.1) and the complexHeatmap package (version 2.0.0)[39]. For enrichment
328 analysis, we used the fgsea[40], the enrichmentbrowser[41], and the Enrichr packages[42].

329

330 Statistical analysis.

331 Each data set was subjected to a normality test prior to further comparisons (Shapiro-Wilk
332 normality test; alpha = 0.05). For normally distributed data sets, a two-tailed unpaired
333 Student's t-test was performed to compare two groups. If more than two groups were analyzed
334 simultaneously, a one-way ANOVA was used followed by appropriate multiple comparison
335 *post hoc* tests to control for multiple comparisons as specified. In case of a non-Gaussian
336 distribution, two-tailed Mann-Whitney tests were used to compare two distinct groups, or a
337 Kruskal-Wallis test followed by Dunn´s *post hoc* test to compare more than two groups. The
338 sample size was determined based on similar experiments carried out in the past and the
339 literature. All plotted data represent mean ± SEM. Statistical analysis was performed using
340 GraphPad Prism 7 (GraphPad Software). All behavioural sessions were video recorded and
341 manually scored to determine the exploration of objects during training and testing phases or
342 freezing behaviour by an experimenter blind to the group identity. The TSE Systems Fear
343 Conditioning program was used to score the mean velocity during the training for CFC.

344

345

346

347

348

349

350

351 **Results**

352

353 **Dnmt3a1 is required for long-term memory formation**

354 In this study, we sought to investigate the role of DNA methyltransferase 3a1 (Dnmt3a1) in
355 neuronal function and memory formation. We employed stereotaxic surgery and recombinant
356 adeno-associated viruses (rAVV) to deliver a control shRNA sequence (Control-shRNA)[3] or
357 two independent shRNAs to knockdown Dnmt3a1 into the adult (8 weeks) dorsal
358 hippocampus (dHPC) of mice (Figure 1A, B). We used the rAAV1/2 serotype given its well
359 established neuronal tropism[43]. To monitor viral expression upon infection, the viral constructs
360 contained a GFP cassette under the control of the chicken-beta-actin promoter (Figure 1A, B).
361 We confirmed knockdown efficiency of our shRNAs by transfection of primary hippocampal
362 neurons *in vitro* and immunostaining against endogenous Dnmt3a1 (Sup Figure 1A). To
363 further validate the knockdown efficiency *in vivo*, we performed qRT-PCR and western blot
364 analysis of dHPC of mice infected with the viral constructs (Sup Figure 1B-G). We confirmed
365 that both sequences selectively knockdown Dnmt3a1 without affecting other *Dnmts*. shRNA1
366 and shRNA2 sequences effectively reduced Dnmt3a1 expression at both the mRNA (Sup
367 Figure 1B, C) and protein (Sup Figure 1D-G) levels. To evaluate a requirement for Dnmt3a1
368 in memory performance, we conducted hippocampus-dependent memory tests on mice three
369 weeks after stereotaxic surgery (Figure 1C). We found that, when tested 24 hours after training
370 in the spatial object recognition test, mice injected with either Dnmt3a1-shRNA1 or -shRNA2
371 exhibited no preference for the displaced object (Figure 1D). However, when evaluated 1 hour
372 after training, mice in shRNA groups explored the displaced object for a length of time
373 comparable to the control group (Figure 1F). Importantly, Dnmt3a1 knockdown did not affect
374 the overall amount of time that mice spent exploring the objects during training (Sup Figure
375 1H, I). To assess further the role of hippocampal Dnmt3a1 in memory formation, we trained
376 mice in contextual fear conditioning. Knockdown of Dnmt3a1 with either shRNA1 or shRNA2
377 impaired contextual fear memory response 24 hours after training (Figure 1E) without
378 decreasing freezing levels compared to the Control-shRNA when tested 1 hour after training
379 (Figure 1G). This decrease in freezing was not due to altered responsiveness to the shock
380 administration during the training session (Sup Figure 1 J, K). These results show that
381 Dnmt3a1 knockdown impairs long-term memory formation without affecting short-term
382 memory.

383 The behavioural testing in this series of experiments was carried out three weeks following
384 stereotaxic delivery of rAAVs to achieve high viral expression and, as a result, high knockdown
385 efficiency. However, the persistent reduction of Dnmt3a1 levels may lead to network-wide
386 changes that could impact learning and memory. Consequently, in order to more directly

387 assign a role for Dnmt3a1 in mature neurons during the process of memory formation, we
388 adopted a temporally controlled method that limited Dnmt3a1 knockdown to the time of
389 behavioural testing. We used a TetON-based system that consisted of two components: for
390 tight control of Tet-dependent transgene expression in neurons, one viral construct contained
391 the human synapsin (hSyn) promoter controlling the expression of the reverse tetracycline-
392 controlled transactivator (rtTA) together with the Tet repressor (TetR) and the fluorescent
393 protein Kusabira Orange (KO) that serves as an infection marker. In the second construct, the
394 Dnmt3a1-specific shRNA sequence 1 or the Control-shRNA was embedded in a microRNA-
395 30-based expression cassette[34], which is under the control of the tetracycline responsive
396 promoter (TRE) (Figure 2A-B). In the absence of doxycycline, TetR is bound to TRE inhibiting
397 its activity. Upon doxycycline administration, TetR releases from the TRE promoter allowing
398 the binding of the activator rtTA. Administration of doxycycline to hippocampal primary cultures
399 verified tight control of transgene expression via the Tet-On system (Sup Figure 2 A-D). The
400 expression of GFP after doxycycline administration increased over a time course of 72 hours
401 (Sup Figure 2B). Western blot analysis of Dnmt3a1 at the same time points revealed a
402 significant knockdown of Dnmt3a1 protein levels at 72 hours (Sup Figure 2C, D). Thus,
403 doxycycline was injected intraperitoneal 72 hours before behavioural testing (Figure 2C). We
404 found that knocking down hippocampal Dnmt3a1 around the time of fear conditioning reduced
405 freezing levels when mice were tested 24 hours after training (Figure 2D), however, mice froze
406 to a similar extent than the control mice when testing occurred 1 hour after training (Figure
407 2E). The responsiveness to the shock administration during the training session did not cause
408 this decrease in freezing (Sup Figure 2E). Taken together, these findings further support a
409 function of Dnmt3a1 during long-term memory formation and suggest that Dnmt3a1
410 participates in the regulation of learning-dependent gene expression required for long-term
411 memory.

412

413 **Dnmt3a1 regulates the expression of activity-dependent genes involved in synaptic**
414 **plasticity**

415 Next, to elucidate the molecular mechanism by which Dnmt3a1 regulates memory
416 consolidation we sought to identify activity-dependent genes regulated by Dnmt3a1. To this
417 end, we performed RNA sequencing of hippocampal neurons infected with Dnmt3a1-shRNA2
418 or a Control-shRNA after inducing neuronal activity by bicuculline treatment (Figure 3A, B,
419 Sup Figure 3A, B). In control conditions, we found that neuronal activity leads to the
420 downregulation of 1981 genes and upregulation of 1935 genes including established activity-
421 regulated genes, e.g., Arc, Fos, Npas4 (Figure 3C, Sup File 1).

422 To identify activity-regulated genes dependent on Dnmt3a1, we focused on genes that are
423 differentially expressed in Dnmt3a1 knockdown versus control conditions upon bicuculline
424 treatment. These included 1241 genes of which 436 were upregulated and 805 downregulated
425 (Figure 3D, Sup File 2). Notably, the expression of classical immediate early genes, such as
426 Arc, Fos, Npas4 was not altered in Dnmt3a1-shRNA conditions (Sup File 2), suggesting that
427 the identified changes are not a result of an overall disruption of neuronal responses. We
428 hypothesised that Dnmt3a1-regulated genes that are involved in memory formation should be
429 both a) activity-regulated and b) differentially expressed in response to Dnmt3a1 reduction.
430 Thus, we overlapped the activity-regulated (Figure 3C, Sup File 1) and the Dnmt3a1-regulated
431 gene sets (Figure 3D, Sup File 2) in order to find potential activity-regulated Dnmt3a1 target
432 genes. This intersection identified 327 candidates (Figure 3E, Sup Figure 3B, Sup File 3).
433 Gene ontology (GO) analysis of the 327 genes yielded a strong enrichment for terms related
434 to structural and functional plasticity, namely *"Regulation of neurotransmitter receptor activity"*,
435 *"Regulation of signaling receptor activity"* and *"Regulation of cell-substrate adhesion"* (Figure
436 3F). This suggests that genes downstream of Dnmt3a1 may play an important role in synaptic
437 plasticity and learning and memory. We confirmed some of the identified Dnmt3a1 target
438 genes in independent biological samples using qRT-PCR (Figure 3G, H). To further rule out
439 the possibility of off-target effects, this validation was performed using the two independent
440 shRNA sequences. We found that the expression of *Alkal2*, *Cacng5*, and *Nrp1* is regulated by
441 neuronal activity and reduced upon Dnmt3a1 depletion achieved by shRNA1 or shRNA2
442 (Figure 3G), whereas *Crhbp, Npy and Trpc6* failed to show a significant effect with one of the
443 shRNA sequences (Figure 3H). *Dnmt3a* encodes for two distinct isoforms Dnmt3a1 and
444 Dnmt3a2, which are differentially regulated by neuronal activity[22,23]. We further investigated
445 whether the two isoforms regulate distinct targets. To test this, we infected primary
446 hippocampal cultures with a previously validated shRNA to reduce Dnmt3a2 levels[23,24] (Sup
447 Figure 3C) and investigated the impact of this manipulation on the expression of the identified
448 Dnmt3a1-regulated genes. Reduction of Dnmt3a2 did not change the expression of *Alkal2*,
449 *Cacng5* or *Nrp1* neither in basal conditions nor upon neuronal activity (Sup Figure 3D). Taken
450 together these findings demonstrate that Dnmt3a1 is required for the regulation of a synaptic
451 plasticity-related transcriptional program and further suggest that the Dnmt3a2 isoform may
452 regulate a distinct gene pool.

453

454 **Neuropilin-1 is a Dnmt3a1 downstream target required for memory formation**

455 Next, we aimed at investigating whether Dnmt3a1 role in memory consolidation requires the
456 activity of identified target genes. Among the genes whose expression is controlled by
457 Dnmt3a1, we focused on neuronal genes which have been identified to be regulated by novel

458 environment exposure in the mouse hippocampus[44]. These included, among others, the
459 previously validated gene Neuropilin-1 (*Nrp1)* (Figure 3G, H). Nrp1 is known to build a complex
460 with Semaphorin 3a (Sema3A) and Plexin A4 and is implicated in signalling pathways
461 regulating neuronal morphology[31,45]. Although it has been demonstrated that this complex is
462 important for AMPA receptor trafficking[46], whether Nrp1 plays a role in hippocampus-
463 dependent memory formation is still unknown. We performed a shRNA-mediated loss-of-
464 function approach to assess the role of Nrp1 in memory formation. We generated two
465 independent shRNA constructs to reduce the expression of *Nrp1* (Figure 4A) and validated
466 their knockdown efficiency *in vivo* after stereotaxic delivery of the viral constructs or a Control-
467 shRNA into the dHPC. We confirmed that Nrp1-shRNA1 and -shRNA2 sequences led to a
468 robust reduction of Nrp1 mRNA levels (Sup Figure 4A, B). Mice were subjected to a
469 hippocampus-dependent behavioural memory task three weeks after viral delivery (Figure
470 4B). Knockdown of Nrp1 with either shRNA resulted in exploration of the displaced object at
471 chance levels (Figure 4C), as well as in decreased freezing responses in the contextual fear
472 conditioning test compared to mice injected with the Control-shRNA (Figure 4D). Notably,
473 Nrp1 knockdown did not affect the overall object exploration time (Sup Figure 4C) or the
474 responsiveness to the shock administration (Sup Figure 4D). In conclusion, this set of
475 experiments uncovered a novel function for Nrp1 in long-term memory formation.

476

477 **Dnmt3a1, but not Dnmt3a2, regulates long-term memory formation via its downstream**
478 **target Nrp1**

479 To evaluate a function of Nrp1 as a downstream effector of Dnmt3a1 during memory
480 formation, we performed a rescue experiment. To this end, we overexpressed HA-tagged
481 Nrp1 or a control protein (LacZ) under the regulation of hSyn promoter together with either
482 Dnmt3a1-shRNA2 or Control-shRNA sequences in the mouse hippocampus (Figure 5A, B).
483 We first confirmed successful overexpression of Nrp1 in the dHPC by western blot analysis
484 (Sup Figure 5A, B). After stereotaxic delivery of the constructs, mice underwent the spatial
485 object recognition task (Figure 5B). The different groups did not exhibit differences in the time
486 spent exploring the objects during the training session (Sup Figure 5C). As shown above, the
487 reduction of Dnmt3a1 levels caused memory impairments which are manifested by the
488 decreased preference for the displaced object (Figure 1D). Strikingly, this impairment was
489 rescued upon Nrp1 overexpression (Figure 5C). Mice that overexpressed Nrp1 and expressed
490 a control shRNA sequence showed memory performance similar to the control group (Figure
491 5C). Taken together, these results demonstrate that Nrp1 acts downstream of Dnmt3a1, is
492 required for memory formation and can per se rescue Dnmt3a1-dependent memory

493 impairments. Thus, indicating that Dnmt3a1 regulates memory formation, at least in part, via
494 its downstream target Nrp1.

495 Our gene expression analysis suggested that the isoforms Dnmt3a1 and Dnmt3a2 regulate
496 distinct genes. Specifically, we showed that Nrp1 expression is regulated by Dnmt3a1, but it
497 is not altered upon knockdown of Dnmt3a2 (Sup Figure 3D). Next, to investigate a specific
498 functional link between Dnmt3a1, Nrp1 and memory formation, we tested if Nrp1
499 overexpression rescues Dnmt3a2-knockdown-dependent memory impairments. We
500 overexpressed HA-tagged Nrp1 with a Dnmt3a2-specific shRNA sequence in the mouse
501 dorsal hippocampus and performed the spatial object recognition task in mice (Figure 5D, E).
502 Importantly, none of the conditions showed differences in overall time exploring the objects
503 during training (Sup Figure 5D). As previously described[23], knockdown of Dnmt3a2 impaired
504 spatial object recognition memory and remarkably, this impairment was not rescued upon
505 Nrp1 overexpression (Figure 5F). This finding shows that the rescue obtained in response to
506 Nrp1 overexpression is not a result of a generalized memory enhancement effect and further
507 supports that Nrp1 acts downstream of Dnmt3a1 but not Dnmt3a2. Thus, this data uncovers
508 a *Dnmt3a* isoform specific mechanism in memory formation.

509
510
511
512
513
514
515
516
517
518
519
520
521
522
523
524
525
526
527
528

529 **Discussion**

530

531 In this study we demonstrated a critical role for Dnmt3a1 in long-term memory formation by
532 showing that acute knockdown of Dnmt3a1 in the adult hippocampus selectively impairs long-
533 term memory formation and further identified activity-dependent genes regulated by Dnmt3a1
534 levels. Furthermore, our data suggests that despite a requirement for both Dnmt3a1 and
535 Dnmt3a2 for memory formation, the two isoforms regulate this process via distinct
536 mechanisms; Nrp1 overexpression rescued Dnmt3a1, but not Dnmt3a2, knockdown-driven
537 impairments in memory formation. Taken together these findings have advanced our
538 understanding of the requirement for distinct Dnmts in mnemonic processes as well as of the
539 identity of downstream effector molecules.

540 Most studies that aimed at investigating the role of Dnmt3a in adult brain cognition have
541 utilized heterozygous constitutive[47] or conditional knock-out mice[15,16,48]. These models delete
542 *Dnmt3a* during critical prenatal and postnatal neurodevelopmental phases, which may
543 confound the interpretation of the function of *Dnmt3a*-coded proteins in memory formation in
544 the adult. Mitchnick and colleagues (2015) used small interfering RNAs to acutely disrupt
545 *Dnmt3a* expression in the adult hippocampus and provided compelling evidence for a role of
546 *Dnmt3a*-coding genes in long-term hippocampal memory formation[14]. In addition, our present
547 and previous studies[23–25] have corroborated these findings and demonstrated that both
548 Dnmt3a isoforms, Dnmt3a1 and Dnmt3a2, are required for memory formation in adult mature
549 neurons. This study has further identified for the first time an activity-regulated genomic
550 program regulated by Dnmt3a1 levels in hippocampal neurons. We found that the knockdown
551 of Dnmt3a1 altered the expression of several genes. Even if counterintuitive at first, the
552 reduction of Dnmt expression resulted not only in de-repression of gene expression, but also
553 downregulation. Although these gene expression changes are likely a combination of direct
554 effects on the altered genes and indirect mechanisms via the disruption of expression of other
555 transcriptional regulatory processes, these findings corroborate previous studies in which a
556 link between transcription activation and DNA methylation has been shown[10,28,49]. In our
557 transcriptomic analysis we found that Dnmt3a1 regulates the expression of several genes with
558 key roles in synaptic plasticity and memory. Namely, we found changes in the expression of
559 *Npy*, *Cort*, *Trpc6*, which have been implicated in memory consolidation[50–52]. Upon the
560 confirmation with two independent shRNA sequences, we focused on Nrp1 which has been
561 shown to be regulated by enriched environment exposure[53] and within dentate gyrus memory
562 engrams[44]. Besides the established function for the semaphorins and their receptors (Nrp and
563 plexin family members) in neurodevelopment[32,54], only a few lines of evidence demonstrated
564 their involvement in homeostatic and Hebbian forms of plasticity in the adult

565 hippocampus[31,46,55,56]. Notably, Nrp1 is localised at synapses of the adult rat hippocampus[56]
566 and secreted semaphorins acting on the sema-Nrp-plexin complex modulate synaptic
567 connectivity in granule cells of dentate gyrus and pyramidal neurons of CA1[56] as well as AMPA
568 receptor trafficking in CA3-CA1 synapses[46]. The present study adds to this body of literature
569 by demonstrating that Nrp1 is required for the formation of hippocampal long-term memory.
570 Intriguingly, we showed that overexpression of hippocampal Nrp1 rescued Dnmt3a1
571 knockdown-dependent memory impairments. Thus, our findings suggest that the regulation of
572 Nrp1-dependent mechanisms during memory consolidation is a mechanism via which
573 Dnmt3a1 contributes to memory formation.

574 This study uncovered a dissociation in the downstream processes regulated by the Dnmt3a
575 isoforms during hippocampal long-term memory formation. Notably, we showed that Nrp1
576 overexpression selectively rescued memory impairments promoted by the reduction of
577 Dnmt3a1, but not Dnmt3a2, levels in the adult hippocampus. Our previous work had already
578 demonstrated differential regulation of the two enzymes upon neuronal activity and learning.
579 In contrast to Dnmt3a1, Dnmt3a2 mRNA levels are induced in response to action potential
580 bursting and learning[23], cocaine administration[30] and an inflammatory response[29] in different
581 regions of the central nervous system. Despite the lack of regulation at the level of
582 transcription, Dnmt3a1 protein levels appear to be regulated upon neuronal activity[22]. It has
583 also been shown that Dnmt3a isoforms target unique genomic loci[21,57]. Collectively, these
584 findings indicate distinct regulatory functions. Specifically, during the formation of memory,
585 lack of redundancy is further supported by our studies that showed that impairments in long-
586 term memory formation promoted by the acute, reduced hippocampal expression of Dnmt3a1
587 or Dnmt3a2 are not compensated by the other isoform. Thus, the emerging picture is that the
588 distinct Dnmts are required for cognitive abilities through the regulation of complementary but
589 non-overlapping processes. The recruitment of Dnmts to DNA is thought to be guided by
590 chromatin marks, namely histone modifications[58] and non-coding RNA species that direct
591 gene-specific methylation patterns[59–63]. Notably, differential DNA recruitment between
592 Dnmt3a1 and Dnmt3a2 may be at least in part driven by distinct recognition of histone tail
593 marks[21,28,64,65]. Moreover, the N-terminus unique to Dnmt3a1 has been shown to confer
594 specific chromatin recognition properties to this isoform[28,65.] Future studies should elucidate
595 the mechanisms that dictate the regulation of distinct downstream targets for Dnmt3a1 and
596 Dnmt3a2 in response to neuronal activity.

597 Our findings highlight the complex and highly regulated role of distinct epigenetic regulators
598 in brain function. The relevance of investigating DNA methylation processes in the nervous
599 system is further underscored by the multiple lines of evidence that demonstrated that DNA
600 methylation dysregulation underlies several pathological conditions, such as

601 neurodevelopmental[66] and neurodegenerative[67] diseases as well as psychiatric conditions[68,69]
602 and chronic pain[70]. Therefore, the elucidation of the regulatory mechanisms controlled by the
603 various epigenetic factors is required to gain further understanding of the pathophysiological
604 mechanisms underlying these conditions.

605

606

607

608

609

610

611

612

613

614

615

616

617

618

619

620

621

622

623

624

625

626

627

628

629

**Acknowledgements**

We thank David V.C. Brito, Kübra Gülmez Karaca and Stefanos Loizou for their critical comments on the manuscript. Celia García-Vilela, Carmen Leibold, Stefanos Loizou, and Benjamin Zeuch for technical support. hSyn-LacZ construct was kindly gifted by Prof. Dr. Daniela Mauceri. This work was supported by the Deutsche Forschungsgemeinschaft (DFG) [grant numbers OL 437/1, OL 437/2, OL 437/3 and OL 437/4 to A.M.M.O.], the Chica and Heinz Schaller Foundation [fellowship and research award to A.M.M.O.], and the Joachim Herz Stiftung [Add-on Fellowships for Interdisciplinary Life Science to J.K.].

**Conflict of Interest**

The authors declare no conflicts of interest.

**Data availability**

The RNA-seq data analyzed in this study is publicly available at the National Center for Biotechnology Information (NCBI) Gene Expression Omnibus (GEO) with the accession number GSE232630.

660 **References**


661 1. Benito, E. & Barco, A. The Neuronal Activity-Driven Transcriptome. *Mol Neurobiol*
662 **51**, 1071–1088 (2015).
663 2. Yap, E. L. & Greenberg, M. E. Activity-Regulated Transcription: Bridging the Gap
664 between Neural Activity and Behavior. *Neuron* vol. 100 Preprint at
665 https://doi.org/10.1016/j.neuron.2018.10.013 (2018).
666 3. Brito, D. V. C., Kupke, J., Karaca, K. G., Zeuch, B. & Oliveira, A. M. M. Mimicking
667 age-associated Gadd45γ dysregulation results in memory impairments in young adult
668 mice. *Journal of Neuroscience* **40**, (2020).
669 4. Alberini, C. M. Transcription Factors in Long-Term Memory and Synaptic Plasticity.
670 *Physiol Rev* **89**, 121–145 (2009).
671 5. Alberini, C. M. & Kandel, E. R. The Regulation of Transcription in Memory
672 Consolidation. *Cold Spring Harb Perspect Biol* **7**, a021741 (2015).
673 6. Cholewa-Waclaw, J. *et al.* The Role of Epigenetic Mechanisms in the Regulation of
674 Gene Expression in the Nervous System. *The Journal of Neuroscience* **36**, 11427–
675 11434 (2016).
676 7. Day, J. J. & Sweatt, J. D. Epigenetic Mechanisms in Cognition. *Neuron* **70**, 813–829
677 (2011).
678 8. Oliveira, A. M. M. DNA methylation: a permissive mark in memory formation and
679 maintenance. *Learning & Memory* **23**, 587–593 (2016).
680 9. Medrano-Fernández, A. & Barco, A. Nuclear organization and 3D chromatin
681 architecture in cognition and neuropsychiatric disorders. *Mol Brain* **9**, 83 (2016).
682 10. Suzuki, M. M. & Bird, A. DNA methylation landscapes: provocative insights from
683 epigenomics. *Nat Rev Genet* **9**, 465–476 (2008).
684 11. Halder, R. *et al.* DNA methylation changes in plasticity genes accompany the
685 formation and maintenance of memory. *Nat Neurosci* **19**, (2015).
686 12. Guo, J. U. *et al.* Neuronal activity modifies the DNA methylation landscape in the
687 adult brain. *Nat Neurosci* **14**, 1345–1351 (2011).
688 13. Miller, C. A. & Sweatt, J. D. Covalent Modification of DNA Regulates Memory
689 Formation. *Neuron* **53**, 857–869 (2007).
690 14. Mitchnick, K. A., Creighton, S., O'Hara, M., Kalisch, B. E. & Winters, B. D.
691 Differential contributions of *de novo* and maintenance DNA methyltransferases to
692 object memory processing in the rat hippocampus and perirhinal cortex - a double
693 dissociation. *European Journal of Neuroscience* **41**, 773–786 (2015).
694 15. Feng, J. *et al.* Dnmt1 and Dnmt3a maintain DNA methylation and regulate synaptic
695 function in adult forebrain neurons. *Nat Neurosci* **13**, 423–430 (2010).
696 16. Morris, M. J., Adachi, M., Na, E. S. & Monteggia, L. M. Selective role for DNMT3a
697 in learning and memory. *Neurobiol Learn Mem* **115**, 30–37 (2014).
698 17. Zocher, S. *et al. De novo* DNA methylation controls neuronal maturation during adult
699 hippocampal neurogenesis. *EMBO J* **40**, (2021).
700 18. Tatton-Brown, K. *et al.* The Tatton-Brown-Rahman Syndrome: A clinical study of 55
701 individuals with de novo constitutive DNMT3A variants. *Wellcome Open Res* **3**, 46
702 (2018).
703 19. Tatton-Brown, K. *et al.* Mutations in the DNA methyltransferase gene DNMT3A
704 cause an overgrowth syndrome with intellectual disability. *Nat Genet* **46**, 385–388
705 (2014).
706 20. Chen, T., Ueda, Y., Xie, S. & Li, E. A Novel Dnmt3a Isoform Produced from an
707 Alternative Promoter Localizes to Euchromatin and Its Expression Correlates with

Activede Novo Methylation. *Journal of Biological Chemistry* **277**, 38746–38754 (2002).

21. Manzo, M. *et al.* Isoform-specific localization of DNMT3A regulates DNA methylation fidelity at bivalent CpG islands. *EMBO J* **36**, 3421–3434 (2017).
22. Bayraktar, G. *et al.* Synaptic control of DNA methylation involves activity-dependent degradation of DNMT3A1 in the nucleus. *Neuropsychopharmacology* **45**, (2020).
23. Oliveira, A. M. M., Hemstedt, T. J. & Bading, H. Rescue of aging-associated decline in Dnmt3a2 expression restores cognitive abilities. *Nat Neurosci* **15**, (2012).
24. Oliveira, A. M. M., Hemstedt, T. J., Freitag, H. E. & Bading, H. Dnmt3a2: A hub for enhancing cognitive functions. *Mol Psychiatry* **21**, (2016).
25. Gulmez Karaca, K. *et al.* Neuronal ensemble-specific DNA methylation strengthens engram stability. *Nat Commun* **11**, (2020).
26. Feng, J., Chang, H., Li, E. & Fan, G. Dynamic expression of de novo DNA methyltransferases Dnmt3a and Dnmt3b in the central nervous system. *J Neurosci Res* **79**, 734–746 (2005).
27. Guo, J. U. *et al.* Genome-wide antagonism between 5-hydroxymethylcytosine and DNA methylation in the adult mouse brain. *Front Biol (Beijing)* **9**, 66–74 (2014).
28. Gu, T. *et al.* The disordered N-terminal domain of DNMT3A recognizes H2AK119ub and is required for postnatal development. *Nat Genet* **54**, 625–636 (2022).
29. Oliveira, A. M. *et al.* Epigenetic control of hypersensitivity in chronic inflammatory pain by the de novo DNA methyltransferase Dnmt3a2. *Mol Pain* **15**, 174480691982746 (2019).
30. Cannella, N. *et al.* Dnmt3a2 in the Nucleus Accumbens Shell Is Required for Reinstatement of Cocaine Seeking. *The Journal of Neuroscience* **38**, 7516–7528 (2018).
31. Carulli, D., de Winter, F. & Verhaagen, J. Semaphorins in Adult Nervous System Plasticity and Disease. *Frontiers in Synaptic Neuroscience* vol. 13 Preprint at https://doi.org/10.3389/fnsyn.2021.672891 (2021).
32. Pasterkamp, R. J. Getting neural circuits into shape with semaphorins. *Nat Rev Neurosci* **13**, 605–618 (2012).
33. Gulmez Karaca, K., Brito, D. V. C., Kupke, J., Zeuch, B. & Oliveira, A. M. M. Engram reactivation during memory retrieval predicts long-term memory performance in aged mice. *Neurobiol Aging* **101**, 256–261 (2021).
34. Stegmeier, F., Hu, G., Rickles, R. J., Hannon, G. J. & Elledge, S. J. A lentiviral microRNA-based system for single-copy polymerase II-regulated RNA interference in mammalian cells. *Proc Natl Acad Sci U S A* **102**, (2005).
35. Zhang, Z. *et al.* Neuronal ensembles sufficient for recovery sleep and the sedative actions of α 2 adrenergic agonists. *Nat Neurosci* **18**, (2015).
36. Brito, D. V. C., Gulmez Karaca, K., Kupke, J., Frank, L. & Oliveira, A. M. M. MeCP2 gates spatial learning-induced alternative splicing events in the mouse hippocampus. *Mol Brain* **13**, 156 (2020).
37. Bray, N. L., Pimentel, H., Melsted, P. & Pachter, L. Near-optimal probabilistic RNA-seq quantification. *Nat Biotechnol* **34**, (2016).
38. Ritchie, M. E. *et al.* Limma powers differential expression analyses for RNA-sequencing and microarray studies. *Nucleic Acids Res* **43**, (2015).
39. Gu, Z., Eils, R. & Schlesner, M. Complex heatmaps reveal patterns and correlations in multidimensional genomic data. *Bioinformatics* **32**, (2016).
40. Korotkevich, G. *et al.* Fast gene set enrichment analysis. *bioRxiv* 060012 (2021) doi:10.1101/060012.

41. Geistlinger, L., Csaba, G. & Zimmer, R. Bioconductor's EnrichmentBrowser: seamless navigation through combined results of set- & network-based enrichment analysis. *BMC Bioinformatics* **17**, 45 (2016).
42. Chen, E. Y. *et al.* Enrichr: Interactive and collaborative HTML5 gene list enrichment analysis tool. *BMC Bioinformatics* **14**, (2013).
43. Xu, R. *et al.* Quantitative comparison of expression with adeno-associated virus (AAV-2) brain-specific gene cassettes. *Gene Ther* **8**, (2001).
44. Jaeger, B. N. *et al.* A novel environment-evoked transcriptional signature predicts reactivity in single dentate granule neurons. *Nat Commun* **9**, (2018).
45. Simonetti, M. *et al.* The impact of Semaphorin 4C/Plexin-B2 signaling on fear memory via remodeling of neuronal and synaptic morphology. *Mol Psychiatry* **26**, (2021).
46. Jitsuki-Takahashi, A. *et al.* Activity-induced secretion of semaphorin 3A mediates learning. *European Journal of Neuroscience* **53**, (2021).
47. Christian, D. L. *et al.* DNMT3A Haploinsufficiency Results in Behavioral Deficits and Global Epigenomic Dysregulation Shared across Neurodevelopmental Disorders. *Cell Rep* **33**, 108416 (2020).
48. Li, J. *et al.* Dnmt3a knockout in excitatory neurons impairs postnatal synapse maturation and increases the repressive histone modification H3K27me3. *Elife* **11**, (2022).
49. Wu, H. *et al.* Dnmt3a-Dependent Nonpromoter DNA Methylation Facilitates Transcription of Neurogenic Genes. *Science (1979)* **329**, 444–448 (2010).
50. Jiang, J. *et al.* Intrahippocampal injection of Cortistatin-14 impairs recognition memory consolidation in mice through activation of sst 2 , ghrelin and GABA A/B receptors. *Brain Res* **1666**, 38–47 (2017).
51. Xie, R. *et al.* AAV Delivery of shRNA Against TRPC6 in Mouse Hippocampus Impairs Cognitive Function. *Front Cell Dev Biol* **9**, (2021).
52. Gøtzsche, C. R. & Woldbye, D. P. D. The role of NPY in learning and memory. *Neuropeptides* **55**, 79–89 (2016).
53. Cao, L. *et al.* VEGF links hippocampal activity with neurogenesis, learning and memory. *Nat Genet* **36**, 827–835 (2004).
54. Kolodkin, A. L. & Tessier-Lavigne, M. Mechanisms and Molecules of Neuronal Wiring: A Primer. *Cold Spring Harb Perspect Biol* **3**, a001727–a001727 (2011).
55. Wang, Q. *et al.* Neuropilin-2/PlexinA3 Receptors Associate with GluA1 and Mediate Sema3F-Dependent Homeostatic Scaling in Cortical Neurons. *Neuron* **96**, 1084-1098.e7 (2017).
56. Sahay, A. *et al.* Secreted Semaphorins Modulate Synaptic Transmission in the Adult Hippocampus. *The Journal of Neuroscience* **25**, 3613–3620 (2005).
57. Sae-Lee, C. *et al.* Genomic targets and selective inhibition of DNA methyltransferase isoforms. *Clin Epigenetics* **14**, 103 (2022).
58. Jurkowska, R. Z. & Jeltsch, A. Enzymology of Mammalian DNA Methyltransferases. in 87–122 (2016). doi:10.1007/978-3-319-43624-1_5.
59. Holz-Schietinger, C. & Reich, N. O. RNA modulation of the human DNA methyltransferase 3A. *Nucleic Acids Res* **40**, 8550–8557 (2012).
60. Mohammad, F. *et al.* Long noncoding RNA-mediated maintenance of DNA methylation and transcriptional gene silencing. *Development* **139**, 2792–2803 (2012).
61. Watanabe, T. *et al.* Role for piRNAs and Noncoding RNA in de Novo DNA Methylation of the Imprinted Mouse *Rasgrf1* Locus. *Science (1979)* **332**, 848–852 (2011).

806 62. Di Ruscio, A. *et al.* DNMT1-interacting RNAs block gene-specific DNA methylation.
807 *Nature* **503**, 371–376 (2013).
808 63. Savell, K. E. *et al.* Extra-coding RNAs regulate neuronal DNA methylation dynamics.
809 *Nat Commun* **7**, 12091 (2016).
810 64. Ooi, S. K. T. *et al.* DNMT3L connects unmethylated lysine 4 of histone H3 to de novo
811 methylation of DNA. *Nature* **448**, 714–717 (2007).
812 65. Suetake, I. *et al.* Characterization of DNA-binding activity in the N-terminal domain
813 of the DNA methyltransferase Dnmt3a. *Biochemical Journal* **437**, 141–148 (2011).
814 66. Pohodich, A. E. & Zoghbi, H. Y. Rett syndrome: disruption of epigenetic control of
815 postnatal neurological functions. *Hum Mol Genet* **24**, R10–R16 (2015).
816 67. De Jager, P. L. *et al.* Alzheimer's disease: early alterations in brain DNA methylation
817 at ANK1, BIN1, RHBDF2 and other loci. *Nat Neurosci* **17**, 1156–1163 (2014).
818 68. Feng, J. & Nestler, E. J. Epigenetic mechanisms of drug addiction. *Curr Opin*
819 *Neurobiol* **23**, 521–528 (2013).
820 69. Nestler, E. J., Peña, C. J., Kundakovic, M., Mitchell, A. & Akbarian, S. Epigenetic
821 Basis of Mental Illness. *The Neuroscientist* **22**, 447–463 (2016).
822 70. Denk, F. & McMahon, S. B. Chronic Pain: Emerging Evidence for the Involvement of
823 Epigenetics. *Neuron* **73**, 435–444 (2012).
824

825

826

827

828

829

830

831

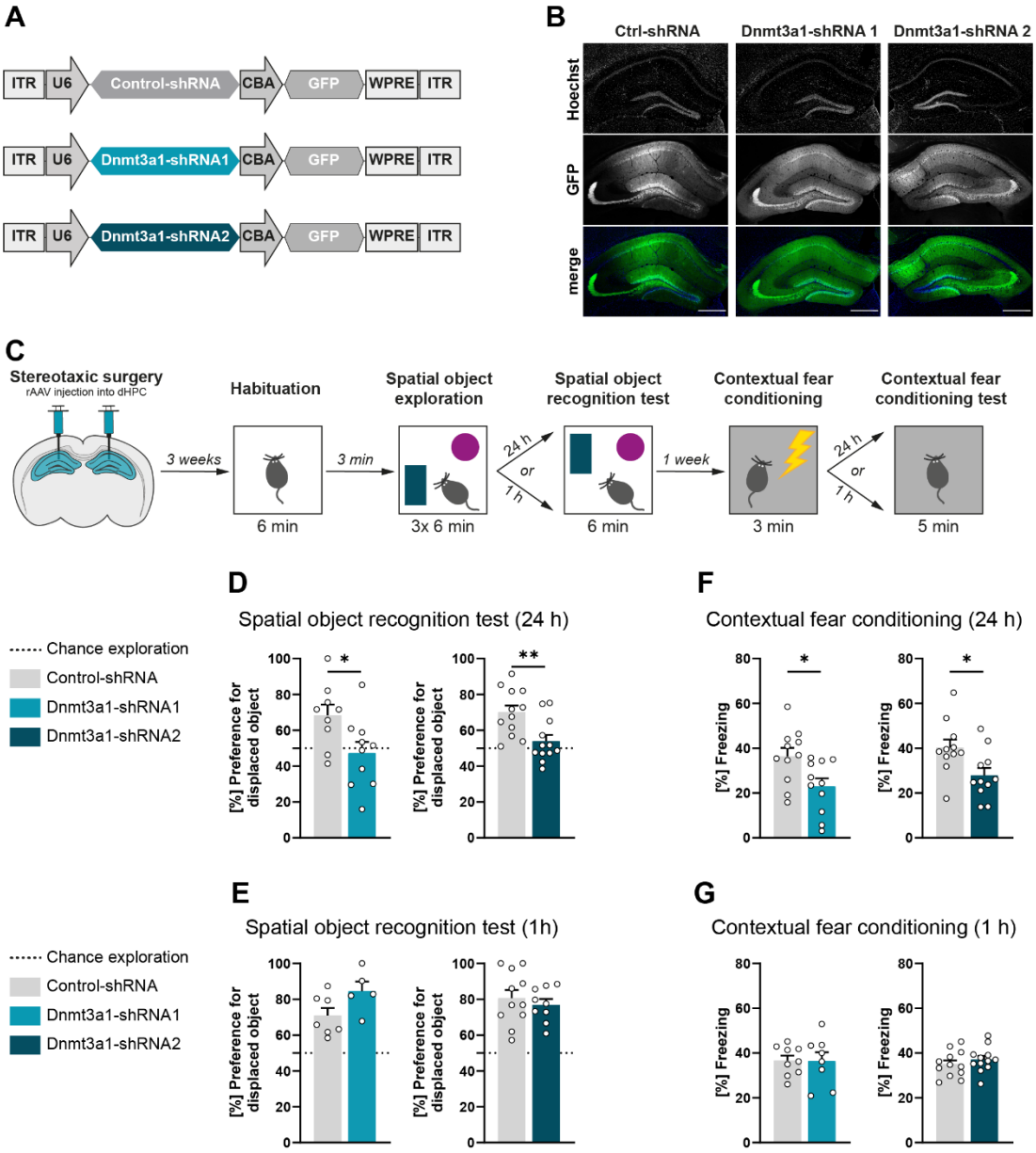


**Figure 1: Reduced hippocampal Dnmt3a1 levels impair memory formation.** (**A**) Schematic representation of viral constructs. (**B**) Representative images of the dorsal hippocampus of mice infected with Control-shRNA, Dnmt3a1-shRNA1 or Dnmt3a1-shRNA2. Scale bar: 100 µm. (**C**) Schematic representation of experimental design. (**D, E**) Long-term (D) or short-term (E) spatial object recognition memory of mice expressing Control-shRNA (n=7-12), Dnmt3a1-shRNA1 (n=5-10) or Dnmt3a1-shRNA2 (n=9-12). Dashed lines represent equal preference for either object (chance exploration). *p<0.05, **p<0.01 by two-tailed, unpaired t-test. (**F, G**) Long-term (F) or short-term (G) contextual fear memory of mice expressing Control-shRNA (n=9-11), Dnmt3a1-shRNA1 (n=8-11) or Dnmt3a1-shRNA2 (n=11-13). *p<0.05 by two-tailed, unpaired t-test.

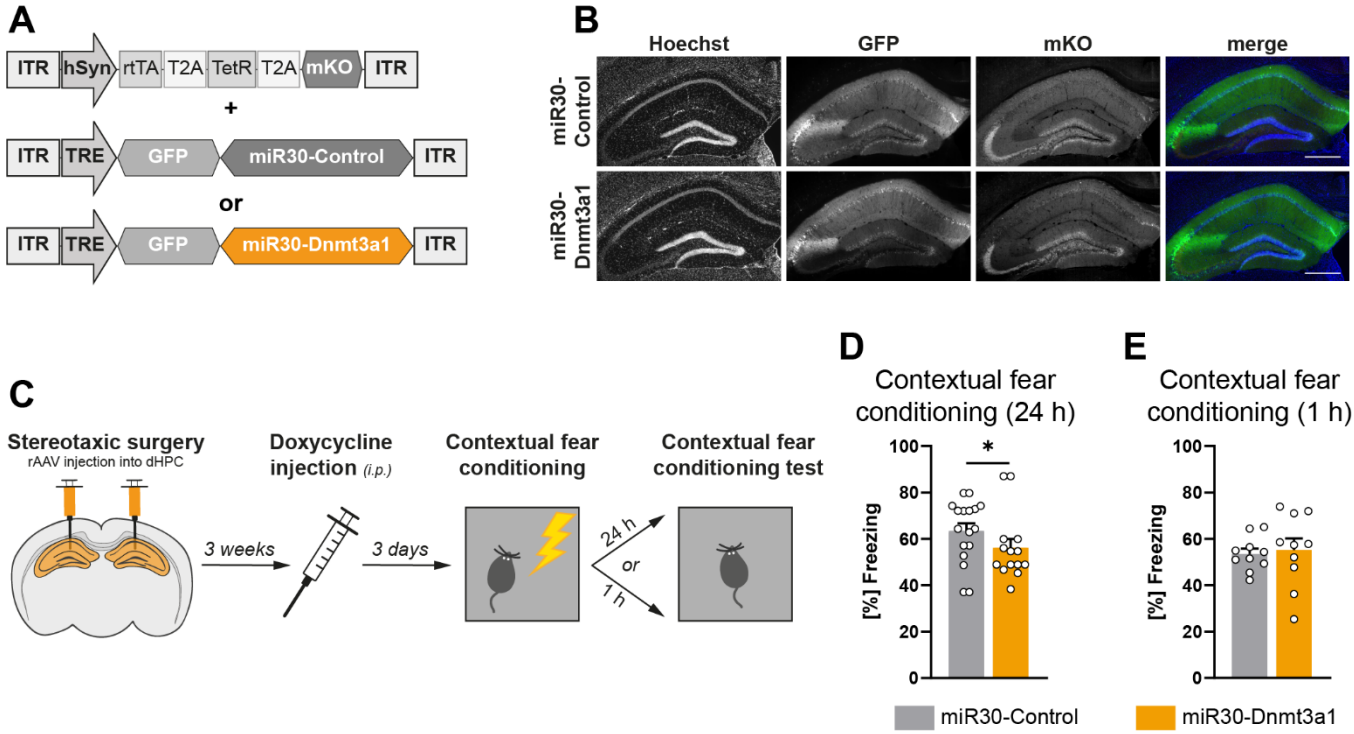


**Figure 2: Temporally-restricted Dnmt3a1 knockdown impairs memory consolidation.** (**A**) Schematic representation of the viral constructs encoding the TetON-based system. The driver construct expresses under the hSyn promoter the Tet repressor (TetR), the reverse tetracycline-controlled transactivator (rtTA) and the infection marker Kusabira Orange (mKO). The Tet response element (TRE)-dependent construct contains the TRE promoter driving the miR30-based shRNA cassettes. In the absence of doxycycline, TRE is inhibited by TetR which results in suppression of the miR30 system. In the presence of doxycycline, TetR loses its affinity thus enabling rtTA to bind to TRE and activate the expression of the miR30 system. (**B**) Representative images of the dHPC of mice infected with rAAVs expressing the miR30-Control shRNA or miR30- Dnmt3a1-shRNA2 sequence. Scale bar: 100 µm. (**C**) Schematic representation of experimental design. (**D, E**) Long-term (D) or short-term (E) contextual fear memory of mice expressing miR30-Control shRNA (n=12-17) or miR30-Dnmt3a1 shRNA (n=10-14). *$p<0.05$, by two-tailed, unpaired t-test.

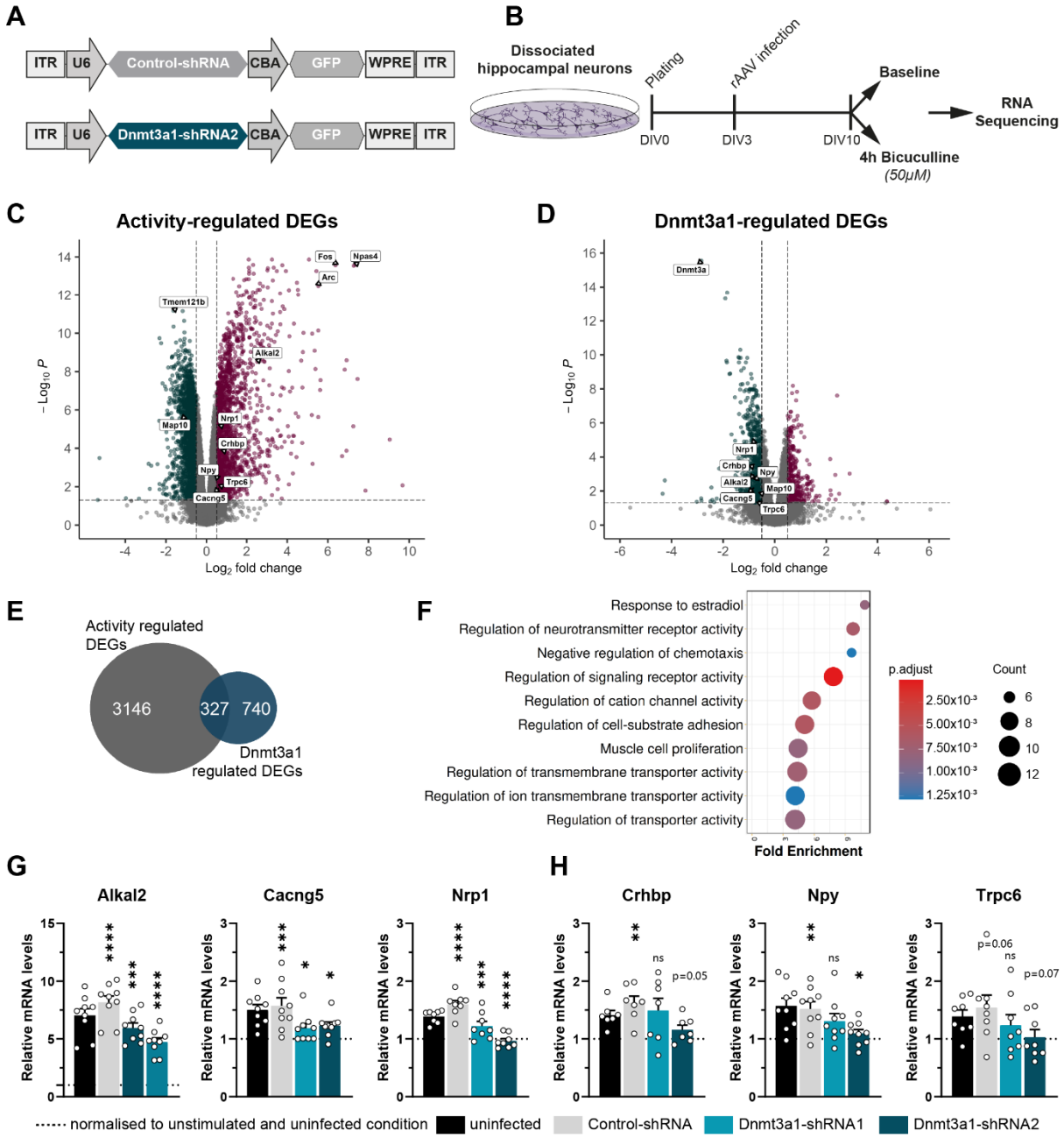


**Figure 3: Dnmt3a1 regulates transcription of genes involved in synaptic plasticity processes.** (**A**) Schematic representation of viral constructs. (**B**) Experimental design used to identify activity-regulated genes whose expression is altered upon Dnmt3a1 reduction. DIV: Day *in-vitro*. (**C**) Volcano plot of differentially expressed genes (DEGs) in control condition (infected with rAAVs expressing Control-shRNA) in response to neuronal activity via Bicuculline treatment; n=4 independent neuronal preparation per condition. Log2 fold change cut-off: ± 0.5; adjusted p-value cut-off: 0.05. (**D**) Volcano plot of DEGs upon infection with Control-shRNA or Dnmt3a1-shRNA2 in stimulated condition (4h Bicuculline); n=4 independent neuronal preparation per condition. Log2 fold change cut-off: ± 0.5; adjusted p-value cut-off: 0.05. (**E**) Venn-Diagram of activity-regulated DEGs (C) and Dnmt3a1-regulated DEGs (D). (**F**)

873 GO-Term analysis of overlapping genes between activity-regulated and Dnmt3a1-regulated
874 DEGs. Dot plot illustrates Top 10 GO term enrichment of biological processes. (**G**) qRT-PCR
875 analysis of Alkal2, Cacng5, Nrp1 expression levels in hippocampal cultures infected with
876 Control–shRNA or Dnmt3a1-shRNA1 or -shRNA2 and stimulated 4h with Bicuculline.
877 Expression levels were normalised to the uninfected controls in baseline conditions (dashed
878 line); (n=8-9 independent neuronal cultures). *$p<0.05$, ***$p\leq0.001$, ****$p\leq0.0001$ by one-way
879 ANOVA test followed by Sidak's multiple comparisons test. (**H**) qRT-PCR analysis of Crhbp,
880 Npy, Trpc6 expression levels in hippocampal-cultured cells infected with Control–shRNA or
881 Dnmt3a1-shRNA1 or -shRNA2 and stimulated 4h with Bicuculline. Expression levels were
882 normalised to the uninfected controls in baseline conditions (dashed line); (n=7-9 independent
883 neuronal cultures). *$p<0.05$, **$p\leq0.01$, ns: not significant by one-way ANOVA test followed by
884 Sidak's multiple comparisons test.

885

886

887

888

889

890

891

892

893

894

895

896

897

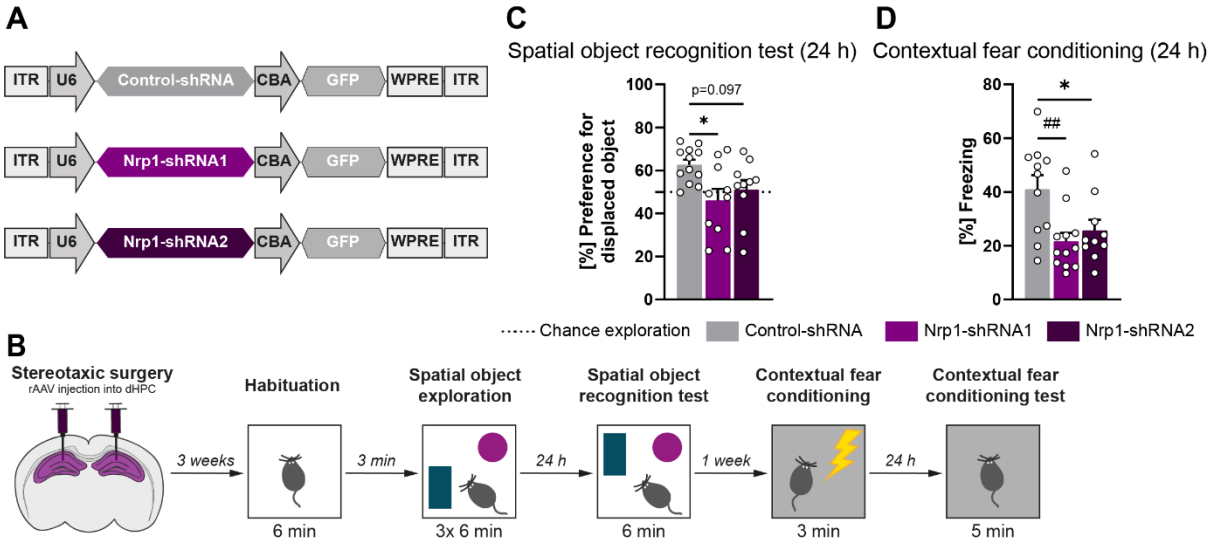


**Figure 4: Hippocampal Neuropilin-1 is required for memory formation.** (**A**) Schematic representation of viral constructs. (**B**) Schematic representation of experimental design. (**C**) Long-term spatial object recognition memory of mice expressing Control-shRNA (n=12), Nrp1-shRNA1 (n=10) or Nrp1-shRNA2 (n=10). Dashed lines represent equal preference for either object (chance exploration). *p<0.05 by one-way ANOVA test followed by Dunnett's multiple comparisons test. (**D**) Long-term contextual fear memory of mice infected with rAAVs expressing Control-shRNA (n=11), Nrp1-shRNA1 (n=12) or Nrp11-shRNA2 (n=10). *p<0.05 by one-way ANOVA test followed by Dunnett's multiple comparisons test. ##p≤0.01 by Kruskal-Wallis test followed by Dunn's multiple comparisons test.

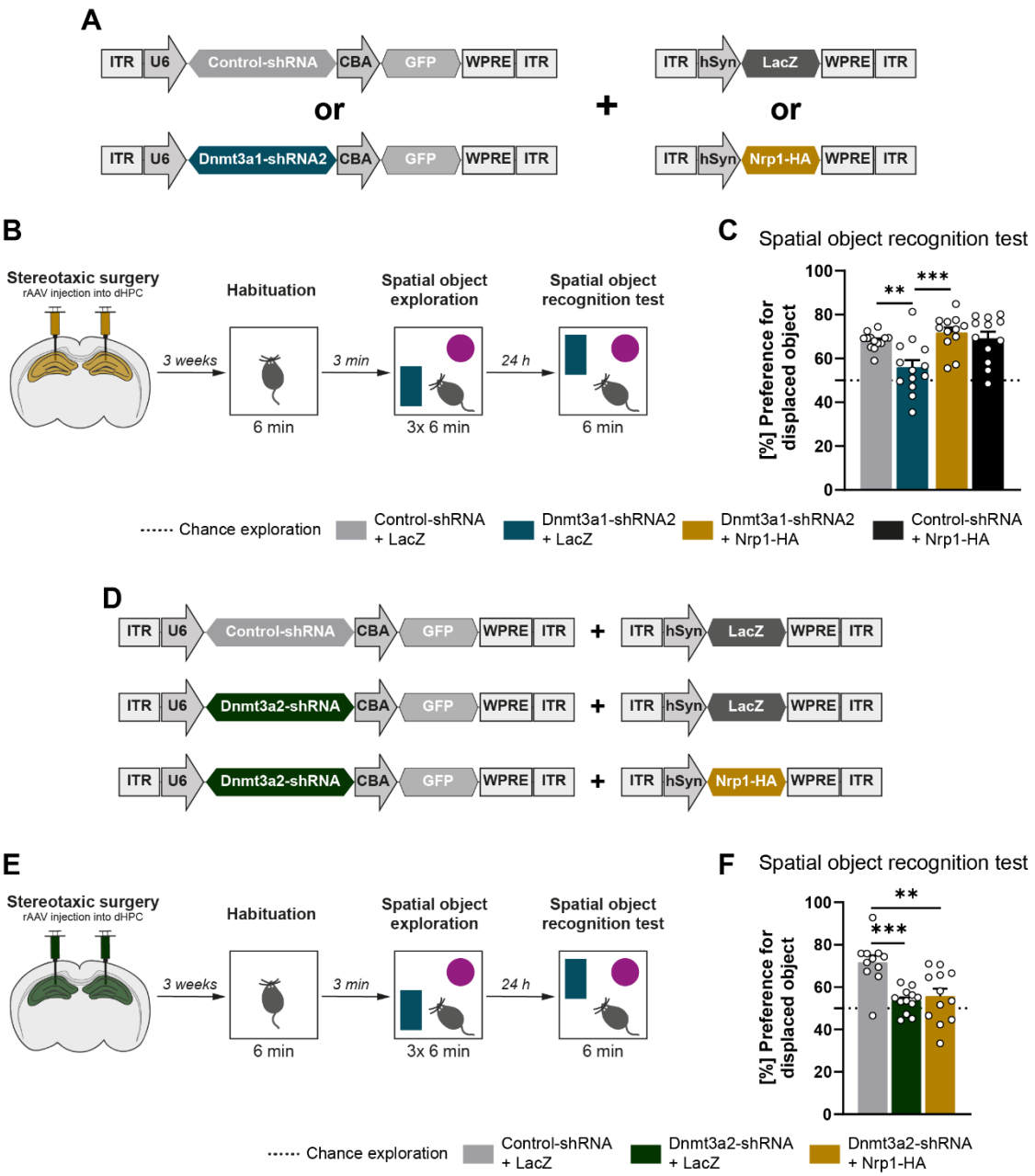


**Figure 5: Neuropilin-1 rescues Dnmt3a1-, but not Dnmt3a2-, dependent memory impairments.** (**A**) Schematic representation of viral constructs. (**B**) Schematic representation of experimental design. (**C**) Long-term spatial object recognition memory of mice expressing Control-shRNA + LacZ (n=13), Dnmt3a1-shRNA2 + LacZ (n=13), Dnmt3a1-shRNA2 + Nrp1-HA (n=12) or Control-shRNA + Nrp1-HA (n=12). Dashed lines represent equal preference for either object (chance exploration). **p≤0.01, ***p≤0.001 by one-way ANOVA test followed by Sidak's multiple comparisons test. (**D**) Schematic representation of viral constructs. (**E**) Schematic representation of experimental design. (**F**) Long-term spatial object recognition memory mice expressing Control-shRNA + LacZ (n=11), Dnmt3a2-shRNA + LacZ (n=12) or Dnmt3a2-shRNA + Nrp1-HA (n=12). Dashed lines represent equal preference for either object

928 (chance exploration). **p≤0.01, ***p≤0.001 by one-way ANOVA test followed by Sidak's
929 multiple comparisons test.

**Sup. Table 1. List of primers used for qRT-PCR.**

| Name | | Sequence |
|---|---|---|
| **Actin** | 5' Primer | TATCCTGACCCTGAAGTACC |
| | 3' Primer | CTCGGTGAGCAGCACAGGG |
| **Alkal2** | 5' Primer | TGAAACATCTCACAGGTCCTCT |
| | 3' Primer | GTGCAGTCTCTCGTGTTGTG |
| **Cacng5** | 5' Primer | CCCTCGTCAGCCTCTTCTTC |
| | 3' Primer | ACCACAAGAGAGAGGCCAGA |
| **Crhbp** | 5' Primer | CTGAAGGTATTTGATGGTTGGA |
| | 3' Primer | TCTTCATAGTGGGCAGAGGG |
| **Nrp1** | 5' Primer | GCAAGACTCGAATCCTCCC |
| | 3' Primer | CCAATGTGAGGGCCAACTTC |
| **Npy** | 5' Primer | CGTGTGTTTGGGCATTCTGG |
| | 3' Primer | TGCCATATCTCTGTCTGGTGA |
| **Trpc6** | 5' Primer | CCAGCTTCCGGGGTAATGAA |
| | 3' Primer | ACATGTATGCTGGTCCTCGA |

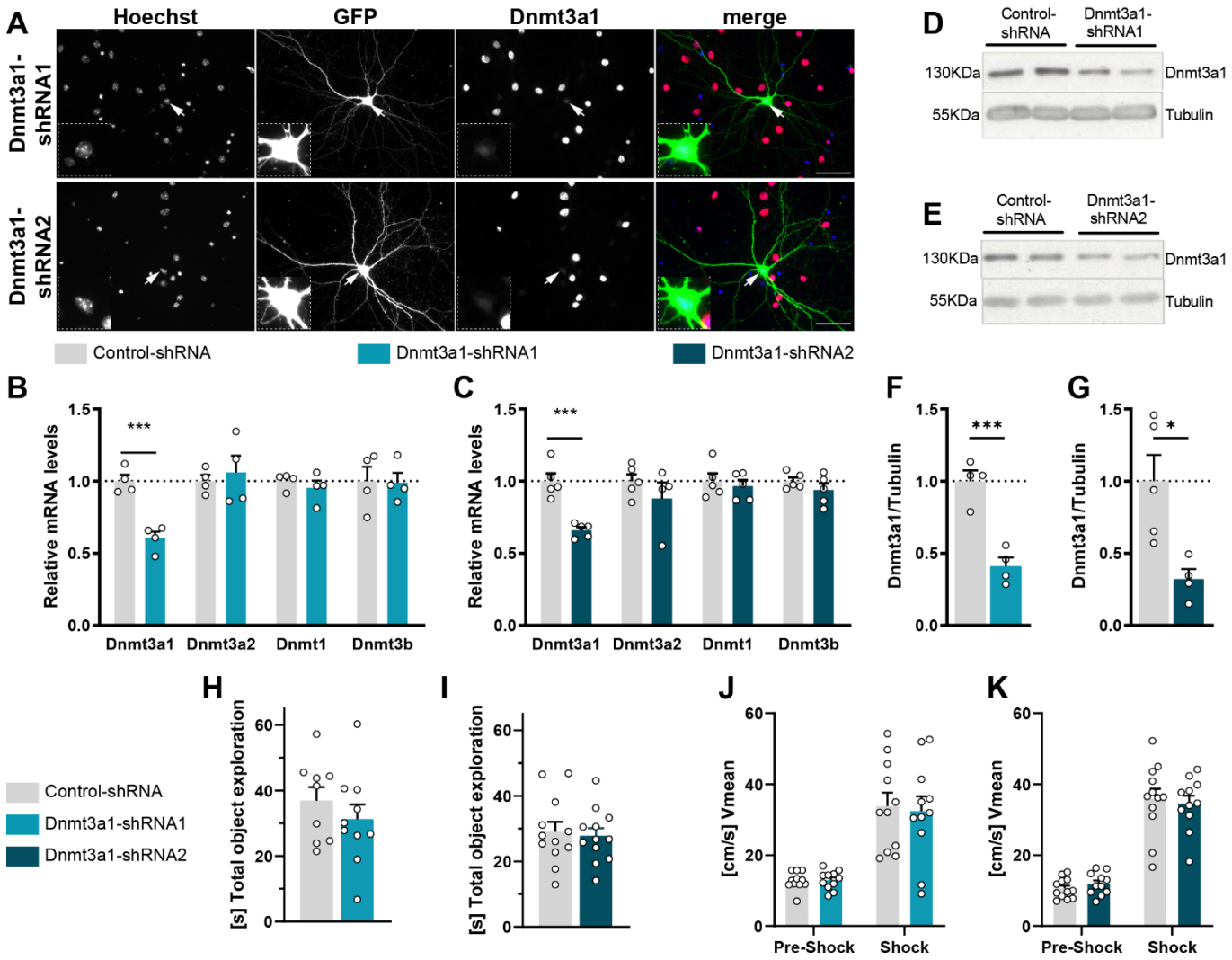


**Sup. Figure 1: Validation of Dnmt3a1 shRNA-dependent knock down and behavioural control parameters.** (**A**) Representative image of primary hippocampal cultures transfected with Dnmt3a1-shRNA1 or Dnmt3a1-shRNA2 (green) and immunostained against endogenous Dnmt3a levels (red). Scale bar: 50 µm. (**B, C**) Quantitative reverse-transcription PCR (qRT-PCR) analysis of the expression of DNA methyltransferases (Dnmt) in the dHPC of mice infected with rAAVs against Control-shRNA (n=4-5) or either (B) Dnmt3a1-shRNA1 (n=4) or (C) Dnmt3a1-shRNA2 (n=4). Dashed lines represent normalised expression levels to Control-shRNA. ***p≤0.001 by two-tailed, unpaired t-test. (**D, E**) Representative immunoblot scans of the expression of Dnmt3a1 or Tubulin in the dHPC of mice infected with rAAVs against Control-shRNA or either (D) Dnmt3a1-shRNA1 or (E) Dnmt3a1-shRNA2. (**F, G**) Immunoblot quantification of Dnmt3a1 protein levels in the dHPC of mice infected with rAAVs against Control-shRNA (n= 4-5) or either (F) Dnmt3a1-shRNA1 (n=4) or (G) Dnmt3a1-shRNA2 (n=4). Dashed lines represent normalised Dnmt3a1 to Tubulin expression of control group. *p<0.05, ***p≤0.001 by two-tailed, unpaired t-test. (**H, I**) Total object exploration time of mice infected with rAAVs against Control-shRNA (n=9-12) or either (H) Dnmt3a1-shRNA1 (n=10) or (I) Dnmt3a1-shRNA2 (n=12) during the three sessions of spatial object recognition training. No significant changes by two-tailed, unpaired t-test. (**J, K**) Mean velocities during CFC training pre-shock (Pre-Shock) or during shock (Shock) administration of the mice expressing rAAVs against Control-shRNA (n=11-13) or either (J) Dnmt3a1-shRNA1 (n=11) or (K) Dnmt3a1-shRNA2 (n=11). No significant changes by two-tailed, unpaired t-test.

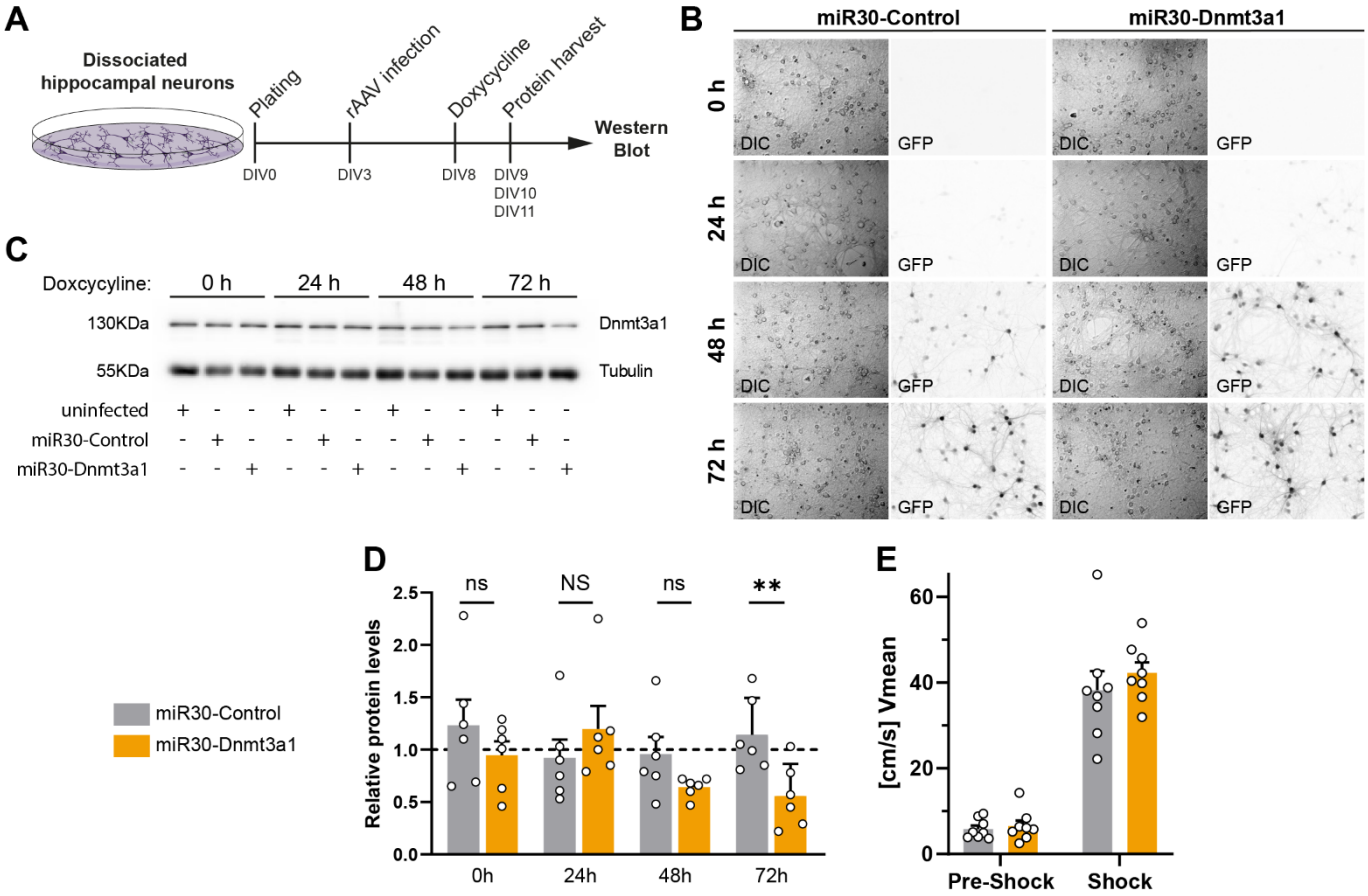


**Sup. Figure 2: Validation of mir30-based Dnmt3a1 shRNA-dependent knock down and behavioural control parameters.** (**A**) Experimental design used to identify the time-point of knock-down using the TetON-based miR30 system. DIV: Day *in-vitro*. (**B**) Representative images of primary hippocampal cells infected with miR30-Control or miR30-Dnmt3a1-shRNA2 sequence. Cultures were treated with doxycycline for 0h, 24h, 48, or 72h. (**C**) Representative immunoblot scans of the expression of Dnmt3a1 and Tubulin of primary hippocampal cultures infected with miR30-Control or miR30- Dnmt3a1-shRNA2 sequence and treated with doxycycline for either 0h, 24h, 48h or 72h. (**D**) Immunoblot quantification of Dnmt3a1 protein levels of primary hippocampal neurons infected with miR30-Control or miR30- Dnmt3a1-shRNA2 sequence and treated with doxycycline for either 0h, 24h, 48h or 72h. Expression levels were normalised to the uninfected controls (dashed line); (n=6 independent neuronal cultures). **p≤0.01, ns: not significant by two-tailed, unpaired t-test. NS: not significant by Mann-Whitney test. (**E**) Mean velocities during CFC training pre-shock (Pre-Shock) or during shock (Shock) administration of the mice expressing miR30-Control (n=8) or miR30-Dnmt3a1 (n=8) shRNAs. No significant changes by two-tailed, unpaired t-test.

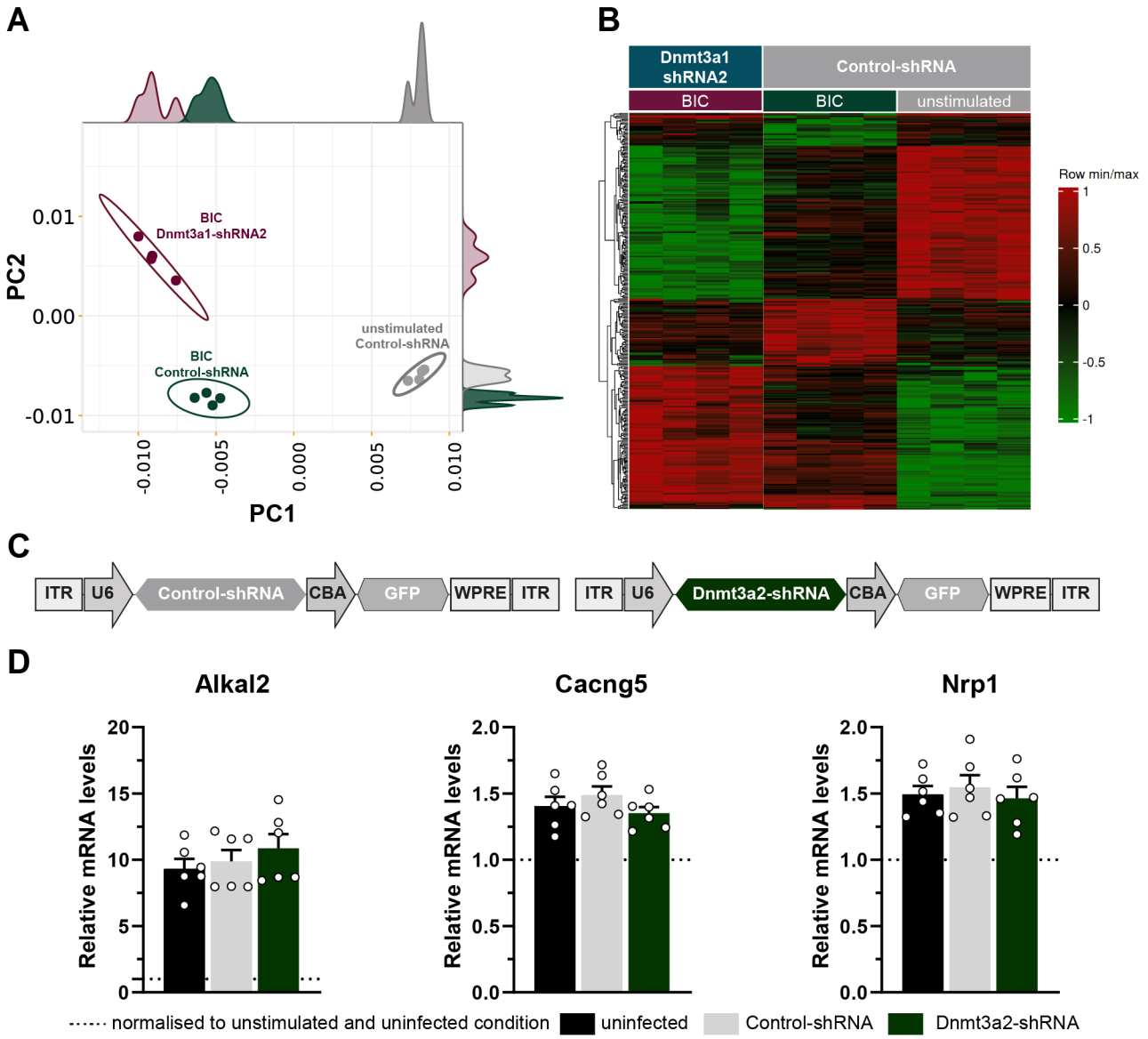


**Sup. Figure 3: PCA analysis and heat map of RNA sequencing data and effect of Dnm3a2 levels on the expression of selected genes.** (**A**) Principle-component analysis (PCA) of DEGs in primary hippocampal cultures infected with Control-shRNA or Dnmt3a1-shRNA2, that were either stimulated with Bicuculline for 4h or unstimulated; (n=4 independent neuronal culture preparations). (**B**) Heatmap of activity-regulated Dnmt3a1-dependent genes (Figure 3E) (n=4 independent neuronal cell preparations). Hippocampal cultures infected with rAAVs expressing Control-shRNA or Dnmt3a1-shRNA2, that were either stimulated with Bicuculline for 4h or unstimulated. (**C**) Schematic representation of viral constructs. (**D**) qRT-PCR analysis of Alkal2, Cacng5 and Nrp1 expression levels in hippocampal-cultured cells infected with Control–shRNA or Dnmt3a2-shRNA and stimulated 4h with Bicuculline. Expression levels were normalised to the uninfected controls in baseline conditions (dashed line); (n=6 independent neuronal cultures). No significant differences between Control-shRNA and Dnmt3a2-shRNA by two-tailed, unpaired t-test.

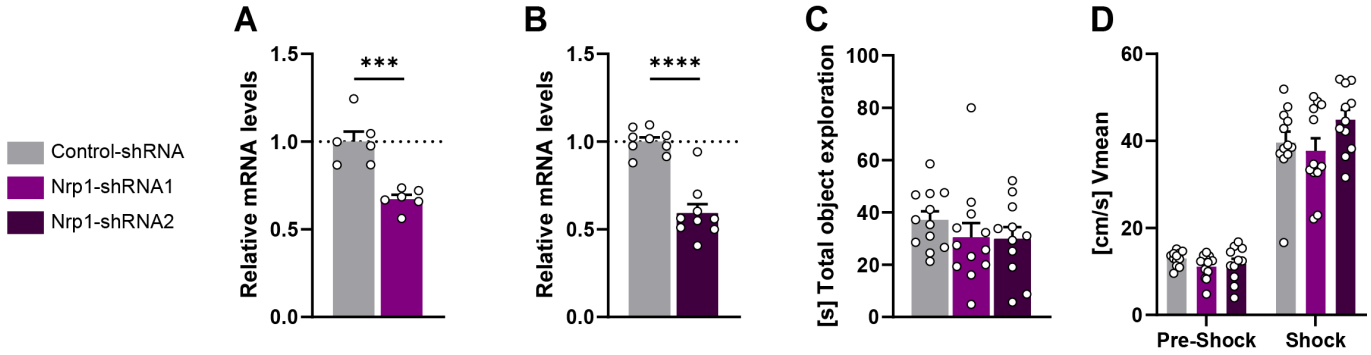


**Sup. Figure 4: Validation of Nrp1 shRNA-dependent knock down and behavioural control parameters.** (**A, B**) qRT-PCR analysis of Nrp1 expression in dHPC of mice infected with rAAVs against Control-shRNA (n=6-9), (A) Nrp1-shRNA1 (n=6) or (B) Nrp11-shRNA2 (n=9). Dashed lines represent normalised expression levels to Control-shRNA. ***p≤0.001, ***p≤0.0001, by two-tailed, unpaired t-test. (**C**) Total object exploration time of mice infected with rAAVs against either Control-shRNA (n=12) or Nrp1-shRNA1 (n=12) or Nrp1-shRNA2 (n=11) during the three sessions of spatial object recognition training. No significant changes between Control shRNA and either Nrp1-shRNA1 or Nrp1-shRNA2 by one-way ANOVA test followed by Dunnett's multiple comparisons test. (**D**) Mean velocities during CFC training pre-shock (Pre-Shock) or during shock (Shock) administration of the mice infected with either Control-shRNA (n=12) or Nrp1-shRNA1 (n=12) or Nrp1-shRNA2 (n=11). No significant changes between Control shRNA and either Nrp1-shRNA1 or Nrp1-shRNA2 by one-way ANOVA test followed by Dunnett's multiple comparisons test.

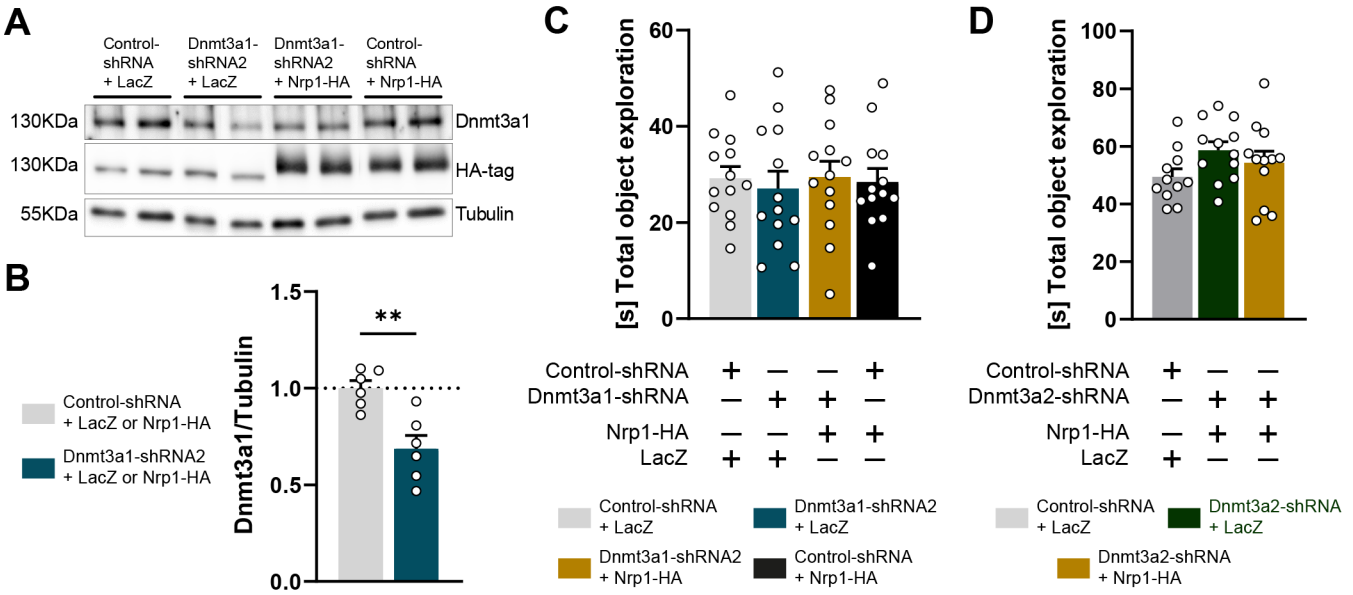


**Sup. Figure 5: Validation of Nrp1 overexpression and behavioural control parameters.** (**A**) Representative immunoblot scans of the expression of Dnmt3a1, HA-tagged Nrp1 or HA-tagged LacZ and Tubulin in the dHPC of mice infected with rAAVs as indicated. (**B**) Immunoblot quantification of Dnmt3a1 protein levels in the dHPC of mice infected with rAAVs against Control-shRNA (n= 6) or Dnmt3a1-shRNA2 (n=6). Dashed lines represent normalised Dnmt3a1 to Tubulin expression of control group. **$p \leq 0.01$ by two-tailed, unpaired t-test. (**C**) Total object exploration time of mice infected with Control-shRNA + LacZ (n=13), Dnmt3a1-shRNA2 + LacZ (n=13), Dnmt3a1-shRNA2 + Nrp1-HA (n=13) or Control-shRNA + Nrp1-HA (n=13) during the three sessions of spatial object recognition training. No significant changes by one-way ANOVA test followed by Sidak's multiple comparisons test. (**D**) Total object exploration time of mice infected with Control-shRNA + LacZ (n=11), Dnmt3a2-shRNA + LacZ (n=12), Dnmt3a2-shRNA + Nrp1-HA (n=12) during three sessions of spatial object recognition training. No significant changes by one-way ANOVA test followed by Sidak's multiple comparisons test.